Saudi Journal of Biological Sciences 26 (2019) 2037–2042

Contents lists available at ScienceDirect

Saudi Journal of Biological Sciences

journal homepage: www.sciencedirect.com

Analysis of the control mechanism of lung cancer of caspase recruitment domain-containing protein 9 and myeloid-derived suppressor cell in Lewis lung cancer mice model

Xiaowei Wu, Fan Li, Yu Deng, Xiaowu Fan *

Department of Thoracic Surgery, Tongji Hospital, Tongji Medical Collage of Huazhong University of Science and Technology, Wuhan 430030, Hubei, China

ARTICLE INFO

Article history:
Received 15 July 2019
Revised 21 September 2019
Accepted 24 September 2019
Available online 24 September 2019

Keywords:
CARD9
IDO
MDSCs
Mouse

ABSTRACT

The purpose of this study was to explore the internal mechanism of lung cancer under the action of caspase recruitment domain-containing protein 9 (CARD9) and immunosuppressive cells myeloid-derived suppressor cells (MDSCs) in the Lewis lung cancer mice model. In this research, mice were selected as research objects, and the mechanism of CARD9 and immunosuppressive cells MDSCs in lung cancer was studied by experimental methods such as mRNA expression level, HE staining of tumor cells, and electron microscopy. The results showed that CARD9 regulated lung cancer by controlling the working state of immunosuppressive cells MDSCs and its downstream product indoleamine 2, 3-dioxygenase (IDO). The study confirmed the tumor regulatory mechanism of CARD9-MDSCs-NF-KB-IDO in MDSCs under tumor environment. In summary, the mechanism of CARD9 and immunosuppressive cells MDSCs in lung cancer was to achieve the goal of tumor control through the control of downstream product IDO. There are still some shortcomings in the research process, but the research results still provide some guidance for future research. Therefore, it is a research topic with practical significance.

1. Introduction

CARD9 is a very important gene protein in the human body, and its role is mainly reflected in connection and signal transmission (Daillère et al., 2016; Roudi et al., 2017). It can play a regulatory and control role on some immunosuppressive cells, and then control the bacterial cells in the human body. Therefore, the study of CARD9 is very important and necessary (Rui et al., 2016; Zhiyu et al., 2016; Alexander et al., 2018). MDSCs, a very important bone marrow immunosuppressive cell in human body, are affected by CARD9, and it can play a very significant role in the working state of MDSCs (He et al., 2018; Li et al., 2018). At present, there are few researches on this aspect, and it is still unknown how the two influence each other. However, it is certain that CARD9 have a very significant effect on the working state of MDSCs (Zhang et al., 2017; Wang et al., 2018). In this research, CARD9′s mechanism of action on MDSCs is studied for lung cancer, hoping to clearly find out how the two cooperate to control the disease. It is believed that the study of such a mechanism is very important for the development of biology and medicine. CARD9-/- mice and WT mice were used as research objects to conduct a detailed study on the status of immune cells in the body, and the research objectives were achieved by means of gene detection, cell staining, microscope observation and other means.

MDSCs were removed by injecting Anti-Gr-1 into the body of the mouse. The number of anti-immune cells MDSCs in the body tumor of CARD9 mice and the number of anti-immune cells MDSCs in the tumor of WT mice under the same treatment conditions was the key to the observation in the experiment (Hotchkiss et al., 2016; Daley et al., 2017; Toubai et al., 2016). And the number of tumor-associated toxic cell T-cell CD8 + T in CARD9-/- mice and the condition of WT mice under the same treatment conditions also needed to be monitored (Singh et al., 2016). The expression of related genes in CARD9 mouse tumors after Anti-Gr-1 injection and WT mice treated under the same conditions were all subject to data analysis (Esser et al., 2018; Qin et al., 2018; Yumin et al., 2017). It can be inferred from the above that CARD9 and immunosuppressive cells MDSCs are very important and significant in the

* Corresponding author.
E-mail address: holiao@yahoo.com (X. Fan).
Peer review under responsibility of King Saud University.

Production and hosting by Elsevier

https://doi.org/10.1016/j.sjbs.2019.09.024
1319-562X/

study of the control mechanism of lung cancer (Jayakumar and Bothwell, 2017; Mackert et al., 2017; Feng et al., 2018).

In summary, the mechanism of CARD9 and the immunosuppressive cells MDSCs in lung cancer was studied by means of mRNA expression level, HE staining of tumor cells, and electron microscopy. The results confirmed that the tumor regulatory mechanism of CARD9-MDSCs-NF-KB-IDO is true in MDSCs in tumor environment, and the goal of tumor control was finally achieved through the control of downstream product IDO. Therefore, it is a research topic of practical significance.

2. Materials and methods

2.1. Experimental objects and instruments

Male 5-year-old C67/B7 mice and male 5-year-old CARD9-/-C67/B7 mice were adopted. The instruments used in the experiment were as follows: fully automatic mild tissue processor (140-073-285) (Miltenyi); autoclave (TOMY); biosafety cabinet (Baker); cell incubator (Thermo Forma); refrigerated centrifuge (Heraeus); ultra-low temperature refrigerator (SANYO); oven (Heraeus); pure water meter; FACS Calibur flow cytometer (BD); CO_2 incubator (ThermoForma); Step One Plus fluorescence ration PCR instrument (ABI); CH2 optical microscope (Olympus); microplate reader (BIO-RAD); nucleic acid level electrophoresis apparatus (Bio-Rad); ultraviolet spectrophotometer (Bio-Rad); Gel Doc EQ MultiImager (Bio-Rad); Step One Plus fluorescence ration PCR instrument (ABI).

2.2. Experiment method

First, the effect of CARD9 on Lewis lung cancer. Creation of the LLC model: 6×10^6 LLC cells (120 μL PBS) were injected subcutaneous into the right half of the mouse body, the volume of space occupied by the mouse tumor was recorded, and the mice were killed on day 21. Preparation of single cell suspension: the tumor and spleen of the mouse were excised and placed in PBS for later use. 2 cm^3 spleen tissue cells were crushed with a syringe. The crushed organs and tissues were blown out with PBS and filtered through a 300-mesh sieve, and the filtrate was cleaned to the centrifuge tube. At 5 °C, 400 g sample was centrifuged for 15 min, supernatant was removed, a certain amount of ACK crack red was added for 3 min, then washed repeatedly with PBS for 3 times, and placed for next use. Single cell suspension of bone marrow: firstly, tibia and ribs of mice were removed. Then the muscles were removed and rinsed repeatedly with PBS solution, from one end to the other, 10 times in a cycle, rinsing the red bone marrow as best as possible. It was blown and cracked red in the centrifugal tube and washed repeatedly with PBS for 3 times, waiting for the next use.

Flow detection: firstly, all the single-cell suspensions in each organ and tissue were put into the corresponding flow tube, 400 g suspensions were centrifuged for 6 min, and supernatant was removed. MDSCs in tumors, bone marrow, spleen, and other external organs: flow antibodies of APC-CD12b and PE-GR-1 were added to each test tube and incubated at 5 °C for 20 min. 2 mL PBS was injected into the test tube for rinsing, followed by centrifugation to remove the supernatant. 300 μL PFA solution with a concentration of 2% was injected and placed in a 3 °C refrigerator for testing within 10 days. Cells in tumors and spleen: the same amount of flow cytometry antibodies of PE-CD3 and FITC-CD8 were injected into each test tube and incubated at 3 °C for 20 min. Then, 1 mL PBS was injected into the test tube for rinsing, followed by centrifugation to remove the supernatant. 300 μL of PFA solution with concentration of 2% was added and placed in a 3 °C refrigerator for testing within 10 days. TAM cells in tumor tissue: in each test tube, APC-anti F4/70 and FITC-CD11b flow antibody were added and incubated at 5 °C for 20 min. 2 mL PBS was injected into the test tube for rinsing and centrifugation was performed to remove the supernatant. 300 μL of PFA solution with concentration of 2% was injected and placed in a 3 °C refrigerator for testing within 10 days.

Total RNA reverse transcription and qPCR: firstly, the proper amount of Trizol was injected into the cell sediments, and the operation was conducted according to the standard experimental procedures. The total RNA of cells was extracted, and then the corresponding cDNA fragments were detected by RT-PCR as required. Reverse transcription system (30 μL): 2 ng RNA, 5ul buffer, 3 μL dNTP, 0.6 μL RNase inhibitor, 0.6 μL Oligo dT, and 0.6 μL ReverTra Ace, and 20–30 μL DEPC was added. Conditions: 43 °C for 30 min, 97 °C for 5 min, and 3 °C for 7 min. The obtained cDNA fragment was subjected to a qPCR operation. ABIStep One Pus fluorescence quantitative PCR instrument was used, and Ct values could be obtained at the same time. Data analysis was conducted in the mode of $2^{-\triangle\triangle Ct}$, with GAPDH as the internal reference. There were 4 replicates for each gene fragment, and 3 holes were established for each sample. Primer sequences are shown in Tables 1 and 2.

Experiments of in vivo removal of MDSCs: LLC tumor model was made before. On the 6th day after the tumor implantation, 300 ng of Anti-Gr-1 or isotype control IgG were injected into the abdominal cavity of the mouse body until half a month, once every 2 days. All mice were sacrificed on day 21 after tumor implantation. After immunohistochemistry, the excised tumor cell tissue was stored in a neutral formaldehyde solution and remained stable.

Ki67 staining: the first step was baking and dewaxing, followed by hydration, and the third step was antigen and repair. The fourth step was to remove endogenous peroxidase, and the fifth step was to seal serum. The sixth step was to wash the serum, then add Ki67, keep the culture at 35 °C in a constant temperature water bath for 30–50 min, and wash it repeatedly with PBS solution for 20 min each time. The seventh step was to add MaxVisionTM and then incubate the liquid C in the kit in a constant temperature bath at 35 °C for 25–30 min. The eighth step was to inject MaxVisionTM, culture the solution D in reagent at 37 °C for 25–35 min in a constant temperature bath, and wash it repeatedly with PBS solution for 20 min each time. The ninth step was the color rendering operation. At the same time of injecting AEC solution, the time was observed and recorded carefully under the microscope, so as to know the time needed for dyeing. The sample was repeatedly rinsed with PBS solution for many times, each time of 20 min. The tenth step was counterstaining, which was repeated with a May hematoxylin shaker for 20–30 s. The eleventh step was to seal the film and use AEC's special color-developing water sealing piece to operate the seal.

Process of HE staining: first, slices that had been treated with distilled water were placed in a solution of hematoxylin water for staining for 10 min. Then, color separation was performed in

Table 1
Primer sequence 1.

Target gene	FP (5′-3′)	RP (5′-3′)
GAPDH	AGGTCGGTGTGAACGGATTTG	GGGGCGTTGATGGCAACA
S100A8	AATCACCAGCCCTCTACAAG	CCCACTTTATCACCATCGCAA
S100A9	ATACTCTAGGAGGAAGGACACC	TCCATATGTCATTTATGAGGGC
P47^{phox}	ACACCTTATTCGCCATATTGC	CCTGCCATTAACCAGGAACA
IDO	TGGCGTATGTGTGGAACCG	CTCGCAGAGGGAACAGCAA
Arg1	CTCCAAGCCAAGTCCTTAGAG	GGAGCGTCATAGGGACATCA
iNOS-2	GTTCTCACCCAACAATACAAGA	GTGGACGGGTCGATGTCAC
gp91^{plox}	TCACATCCCTACCAAAACC	CCTTTTTTTTCCCATTCT

Table 2
Primer sequence 2.

Target gene	FP (5′-3′)	RP (5′-3′)
GAPDH	AGGTCGTGTGAACGGATTTG	GGGGTCGTGATGGCAACA
S100A8	AAACACCATGCCTCTACAAG	CCCACTTTATCACCATCGCAA
S100A9	ATACTCTAGGAGGAAGGACACC	TCCATGATGCATTTATGAGGG
$P47^{phox}$	ACACCTTCATCGCCAATTGC	CCTGCCCTTACCAGGAACA
IDO	TGGCGTATGTGTGAACCG	CTCGCAAGGGAACAGCAA
Arg1	CTCCAAGCAAAGTCCTTAGAG	GGAGCGTCATTAGGGACATCA
iNOS-2	GTTCTCAGCCAACAATACAAGA	GTGGAGGGTCGATGTCAC
$gp91^{plox}$	TCACATCTCTACCAAAACC	CCTTATTTTTCCCCATTCT

acid water and ammonia water, each lasting 5 s. After 2 h of repeated washing with purified water, it was placed in distilled water for 1 min. Dehydration was performed using 70% and 90% alcohol, each group lasting 20 min. The sample was fully stained with Eosin staining solution for 2–5 min. The stained slices were dehydrated under the action of pure alcohol, and the slices were allowed to be transparent under the action of xylene. The transparent slices were added with unique chicle of Canada and sealed with glass slices. After the gum was slightly dried, it could be used by labeling it.

Secondly, study on the internal mechanism of CARD9 and MDSCs in controlling lung cancer. Culture method of primary MDSCs: a single cell suspension based on bone marrow cells of mouse was placed in a 20 mL culture container. Then IL-6 and GM-CSF cytokines with a concentration of 40 ng/mL were injected and cultured in an incubator at a temperature of 35 °C for 6 days and placed for use. Flow detection: firstly, MDSCs were pooled and put into flow tubes. Flow antibodies with similar amounts of APC-CD12b and PE-GR-1 were added into each test tube and incubated at 5 °C for 20 min. Then 2 mL PBS was injected into the tube for rinsing. Centrifugation was performed to remove the supernatant and 300 μL PFA solution with a concentration of about 2% was injected and placed in a refrigerator at 3 °C for testing within 10 days.

MDSCs inhibition experiment: first of all, normal murine organ tissues were obtained and single-cell suspension was prepared. All T cells from the spleen of mice were cultured under the same conditions according to the volume ratios of 1:1, 5:1, and 10:1 respectively with MDSCs that had been isolated and purified. The nutrition system was injected with 1 ng/mL anti-cd3 experimental antibody, which was co-cultured under the same conditions for 4 days, and its reproduction was detected by isotope labeling. Collection of tumor cell culture supernatant: the experimental cells of LLC were cultured in a 5 cm culture container for 5 days, and the supernatant produced was collected and placed. The 200 g sample was centrifuged for 3 min, and the supernatant generated was collected, placed in a 50 mL centrifuge tube, and stored in a refrigerator at −70 °C.

Ki67 staining: the first step was baking and dewaxing, the second step was hydration, and the third step was antigen and repair. The fourth step was to remove endogenous peroxidase, and the fifth step was to seal serum. The sixth step was to wash the serum, then add Ki67, keep the culture at 35 °C in a constant temperature water bath for 30–50 min, and wash it repeatedly with PBS solution for 20 min each time. The seventh step was to add MaxVisionTM and then incubate the liquid C in the kit in a constant temperature bath at 35 °C for 25–30 min. The eighth step was to inject MaxVisionTM, culture the solution D in reagent at 37 °C for 25–35 min in a constant temperature bath, and wash it repeatedly with PBS solution for 20 min each time. The ninth step was the color rendering operation. When injecting AEC solution, the time was observed and recorded carefully under the microscope, so as to know the time needed for dyeing. The sample was repeatedly rinsed with PBS solution for many times, each time of 20 min. The tenth step was counterstaining, which was repeated with a May hematoxylin shaker for 20–30 s. And the eleventh step was to seal the film and use special AEC color-developing water sealing piece to operate the seal.

RNA interference experiment: transfection was performed simultaneously with the differentiation of MDSCs, and micropoly transfection reagent was used. For this experiment, bone marrow cells should be cultured in a culture container 2 days in advance, and corresponding cytokines should be added. The siRNA targeted at NIK mRNA sequences and the required transfection reagent were proportioned according to the required ratio. It was repeatedly blown with pipettor until it was evenly, and incubated for 15 min while maintaining room temperature. The cultivated mixture was added to the cells of the experiment, gently stirred, and placed in an incubator to continue the cultivation. Waiting for 48 h after the transfection operation, the cells of the experiment were subjected to a conventional liquid exchange operation.

Expression level of Western blot protein: firstly, the cells were collected into the EP experimental tube without the enzyme, 400 g cells were centrifuged for 6 min, the upper suspension liquid was removed, and 100 μL lysate was injected respectively. It was shaken at 3 °C for 20 min, then centrifuged at 10,000 rpm for 5 min. The supernatant was taken to another enzyme-free EP experimental tube, and the protein concentration was detected by the BA method. Each experimental sample needs to take 120 ng of protein for later use. 5xloading buffer was added and kept at 96 °C in metal bath for 15 min. SDS-PAGE gel electrophoresis: 90 V of concentrated gel and 110 V of separation glue. Transfer membrane: wet transfer method, after 100 V constant pressure membrane transfer for 60 min, the protein was transferred to 0.45 μm PVDF membrane. Sealing: PVDF membrane was placed in 5% BSA after membrane conversion and sealed for 2 h at room temperature. Primary antibody incubation: TBST was used to wash the membrane to remove the unbound BSA, the primary antibody was diluted according to the antibody specification, PVDF membrane was completely immersed in the primary antibody, and the shakable table was used for incubation overnight at 4 °C. Secondary antibodies incubation: TBST was used to wash the membrane for 4 times, each time for 10 min. After that, HRP-secondary antibody was diluted with 5% BSA, PVDF membrane was completely immersed in the secondary antibody, and incubated in a shaking table at room temperature for 2 h. ECL chemiluminescence development: TBST was used to wash the membrane for 4 times, each time for 10 min. After that, the newly configured luminous solution was added to the membrane, and the Fluor Chem imager was used for imaging and photographing.

3. Results and discussion

The statistical results of MDSCs and CD8 + T cells in tumors of mice with different treatments are shown in Figs. 1 and 2. The changes in immune cells in the body of CARD9-/- mice and WT mice can be observed from the figure. When Anti-Gr-1 was injected into the body of mice to remove MDSCs, the number of anti-immune cells MDSCs in the tumor of CARD9 mice decreased, and the number of anti-immune cells MDSCs in the tumor of WT mice was basically the same under the same treatment conditions. However, the number of tumor-associated toxic T cells CD8 + T increased in CARD9-/- mice, which was basically the same in WT mice with the same treatment. It was found that the expression of related genes in tumors of CARD9 mice decreased after the injection of Anti-Gr-1, which was basically the same as that of WT mice treated under the same conditions. Therefore, it can be concluded that the difference of MDSCs expression between CARD9 mice and

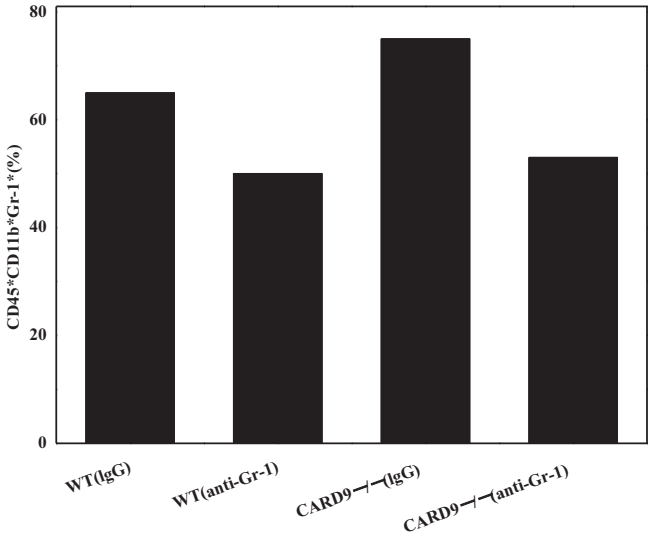

Fig. 1. Statistical results of MDSCs and CD8 + T cells in in tumors of differently treated mice (T-MDSC).

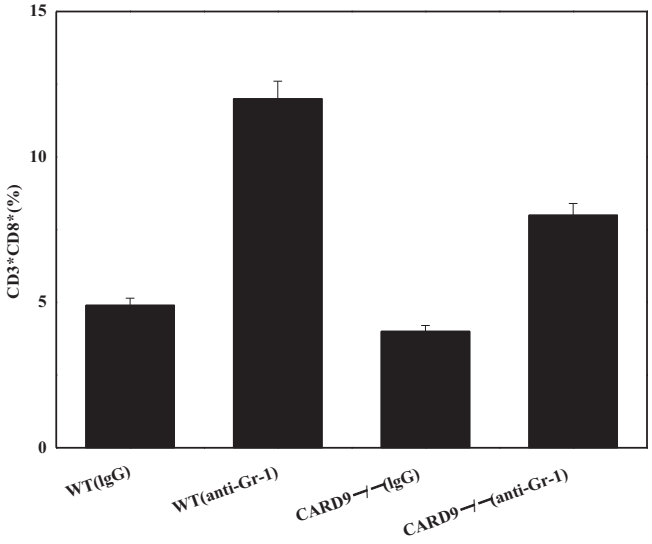

Fig. 2. Statistics results of MDSCs and CD8 + T cells in tumors of differently treated mice (T-CD8).

WT mice can be reduced by removing the anti-immune cells MDSCs.

Changes of tumor differences between CARD9-/- mice and WT mice after intraperitoneal injection of Anti-Gr-1 is shown in Fig. 3. When Anti-Gr-1 was injected into mice to remove MDSCs, the rate of tumor growth in CARD9-/- mice decreased, and the tumor-related differences between CARD9-/- mice and WT mice were reduced after the expression of MDSCs. Therefore, it can be predicted that the removal of anti-immune cells MDSCs can slow the continuous severity of tumor in CARD9 mice.

The expression of MDSCs-related functional genes in spleen and tumor tissues is shown in Figs. 4 and 5. As can be observed from the figure, the expression of iNOS, Gp91phox and IDO genes in the tumors of CARD9 mice was significantly increased compared with that of WT mice, and the expression levels of iNOS and arg-1 genes in the spleen organs of CARD9 mice were significantly increased compared with that of WT mice. Therefore, it can be concluded that CARD9 protein can significantly change the related genes of anti-immune cells MDSCs.

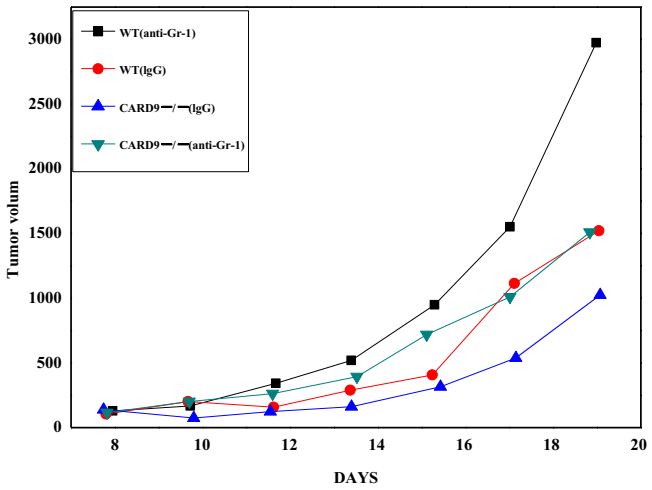

Fig. 3. Changes of tumor differences between CARD9-/- mice and WT mice after intraperitoneal injection of Anti-Gr-1.

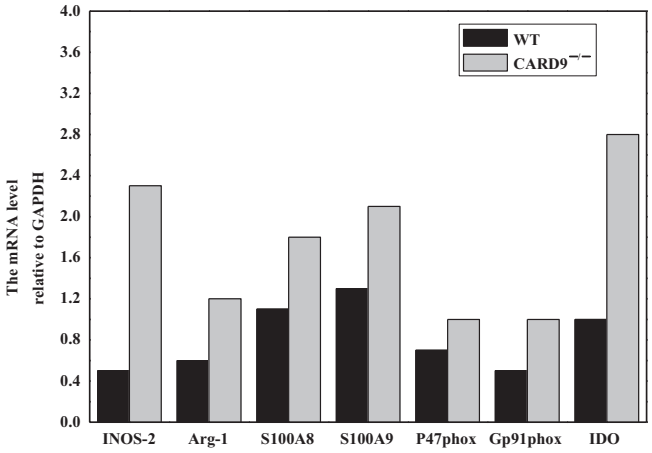

Fig. 4. Expression of MDSCs-related functional genes in tumor tissues.

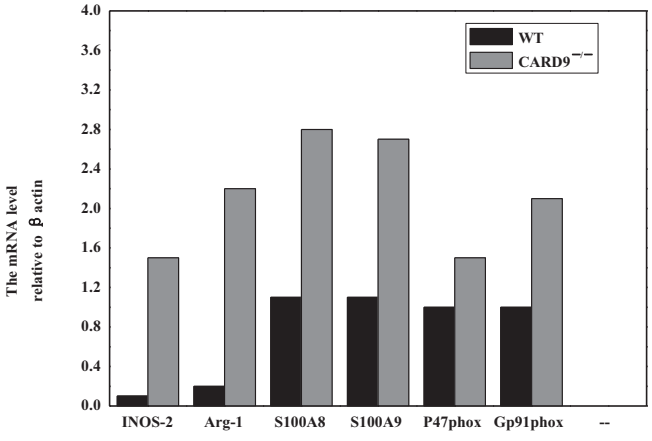

Fig. 5. Expression of MDSCs-related functional genes in spleen tissues.

HE staining and immunohistochemical Ki67 staining of tumor tissues of CARD9-/-murine and WT mice are shown in Fig. 6. It can be clearly observed from the figure that the number of Ki67

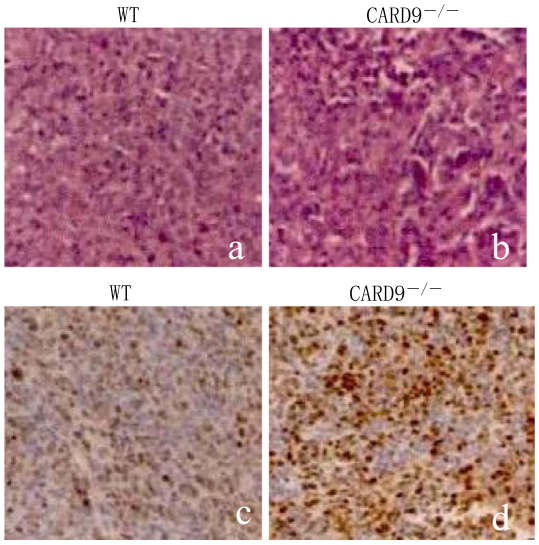

Fig. 6. HE staining and immunohistochemical Ki67 staining of tumor tissues of CARD9-/-murine and WT mice.

positive cells in the tumor cells of CARD9 mice was obviously higher than that in the tumor cells of WT mice, indicating that the growth of tumor cells in CARD9-/- mice was significant. HE staining also showed that there were more bacterial cells in the tumor tissue fragments of CARD9-/- mice.

Expression level of product IDO in MDSCs after si-RNA3 transfection is shown in Fig. 7. In the figure, it can be clearly observed that the non-classical NF-KB pathway of initial MDSCs in CARD9-/- mice can be activated under the action of tumor supernatant through intervention experiments. Through experimental tests, the expression level of the downstream product IDO of the non-classical NF-KB pathway was also observed. It can be observed that expression level of IDO of initial MDSCs in CARD9-/- mice decreased significantly after the action of si-RNA-3 compared with that of WT mice.

Differentiation and function of MDSCs regulated by CARD9 in tumor microenvironment is shown in Fig. 8. It can be clearly observed from the figure that under the action of LLC supernatant, the expression levels of iNOS-2, Arg-1, S100A8/A9, GP91phox and IDO in the initial MDSCs of CARD9 mice were significantly higher than those of WT mice. The isolated and purified CARD9 or the primary anti-immune cell MDSCs of WT mice were cultured at a ratio

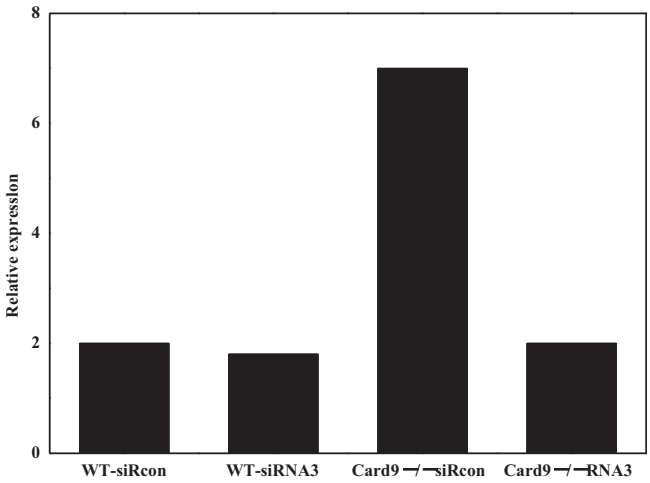

Fig. 7. Expression level of product IDO in MDSCs after si-RNA3 transfection.

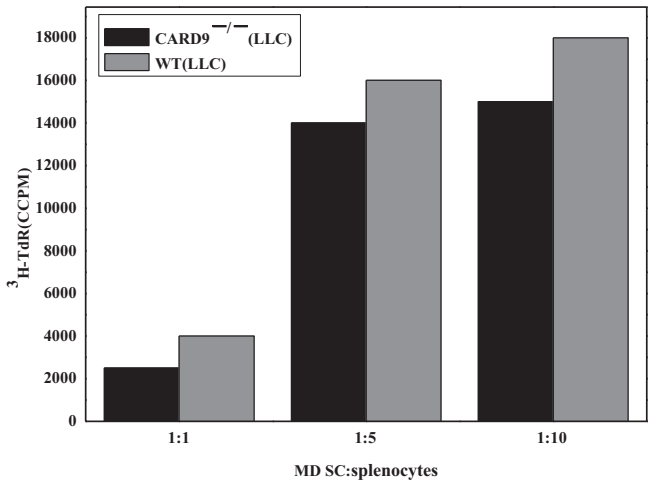

Fig. 8. Differentiation and function of MDSCs regulated by CARD9 in tumor microenvironment.

of 1:1, 5:1, and 10:1. The results showed that the initial anti-immune cells MDSCs in CARD9-/- mice under the action of LLC supernatant had a very significant inhibitory effect on the growth of T cells, and the initial anti-immune cells MDSCs in CARD9-/- mice without the action of LLC supernatant had no significant effect in the growth of T cells. Therefore, it can be concluded that the effect of tumor supernatant can indeed improve the immune function of MDSCs in CARD9 mice.

4. Conclusion

In order to explore the control mechanism of CARD9 and immunosuppressive cells MDSCs in the Lewis lung cancer mice model, mice were selected as research objects in this experiment. The mechanism of CARD9 and immunosuppressive cells MDSCs in lung cancer was studied by experimental methods such as mRNA expression level, HE staining of tumor cells, and electron microscopy. The results showed that CARD9 regulated lung cancer by controlling the working state of immunosuppressive cells MDSCs and its downstream product IDO. The results confirmed the tumor regulatory mechanism of CARD9-MDSCs-NF～KB-IDO in MDSCs under tumor environment. To sum up, the mechanism of CARD9 and immunosuppressive cells MDSCs in lung cancer was to achieve the goal of tumor control through the control of downstream product IDO. There are still some deficiencies in the research process, mainly due to the limited number of samples used in the experiment and the differences between organ and tissue morphology of mice and human body, but the research results still provide some guidance for future research. Therefore, it is a research topic of practical significance.

Acknowledgement

This work was supported by National Natural Science Foundation of China (81700174 and 81802160).

References

Alexander, M.P., Fiering, S.N., Ostroff, G.R., et al., 2018. Beta-glucan-induced inflammatory monocytes mediate antitumor efficacy in the murine lung. Cancer Immunol. Immunother. 67 (11), 1731–1742.
Daillère, R., Vétizou, M., Waldschmitt, N., et al., 2016. Enterococcus hirae and Barnesiella intestinihominis facilitate cyclophosphamide-induced therapeutic immunomodulatory effects. Immunity 45 (4), 931–943.

Daley, D., Mani, V.R., Mohan, N., et al., 2017. Dectin 1 activation on macrophages by galectin 9 promotes pancreatic carcinoma and peritumoral immune tolerance. Nature medicine 23 (5), 556.

Esser, C., Lawrence, B., Sherr, D., et al., 2018. Old receptor, new tricks—the ever-expanding universe of aryl hydrocarbon receptor functions. Report from the 4th AHR Meeting, 29–31 August 2018 in Paris, France. Int. J. Mole. Sci. 19 (11), 3603.

Feng, P.H., Yu, C.T., Chen, K.Y., Luo, C.S., Wu, S.M., Liu, C.Y., et al., 2018. S100a9+ mdsc and tam-mediated egfr-tki resistance in lung adenocarcinoma: the role of relb. Oncotarget 9 (7), 7631–7643.

He, Q., Fu, Y., Tian, D., et al., 2018. The contrasting roles of inflammasomes in cancer. Am. J. Cancer Res. 8 (4), 566.

Hotchkiss, R.S., Moldawer, L.L., Opal, S.M., et al., 2016. Sepsis and septic shock. Nat. Rev. Dis. Primers 2, 16045.

Jayakumar, A., Bothwell, A.L.M., 2017. Stat6 promotes intestinal tumorigenesis in a mouse model of adenomatous polyposis by expansion of mdscs and inhibition of cytotoxic cd8 response. Neoplasia 19 (8), 595–605.

Li, M., Lai, X., Zhao, Y., et al., 2018. Loss of NDRG2 in liver microenvironment inhibits cancer liver metastasis by regulating tumor associate macrophages polarization. Cell Death Dis. 9 (2), 248.

Mackert, J.R., Qu, P., Min, Y., Johnson, P.F., Yang, L., Lin, P.C., 2017. Dual negative roles of c/ebpα in the expansion and pro-tumor functions of mdscs. Sci. Rep. 7 (1), 14048.

Qin, F.Z., Xin, Y.T., Xin, Y.T., Jie, T., Yue, Z., Jie, M., et al., 2018. Lncrna malat1 negatively regulates mdscs in patients with lung cancer. J. Cancer 9 (14), 2436–2442.

Roudi, R., Mohammadi, S.R., Roudbary, M., et al., 2017. Lung cancer and β-glucans: Review of potential therapeutic applications. Invest. New Drugs 35 (4), 509–517.

Rui, K., Tian, J., Tang, X., et al., 2016. Curdlan blocks the immune suppression by myeloid-derived suppressor cells and reduces tumor burden. Immunol. Res. 64 (4), 931–939.

Singh, A., Lelis, F., Braig, S., et al., 2016. Differential regulation of myeloid-derived suppressor cells by Candida species. Front. Microbiol. 7, 1624.

Toubai, T., Mathewson, N.D., Magenau, J., et al., 2016. Danger signals and graft-versus-host disease: current understanding and future perspectives. Front. Immunol. 7, 539.

Wang, Z., Wang, N., Zheng, Y., et al., 2018. Inflammasome and Cancer, Inflammasomes: Clinical and Therapeutic Implications. Springer, Cham, pp. 281–302.

Yumin, W., Yulan, Y., Zhaoliang, S., Qingli, B., Xiaobo, C., Amoah, B.P., et al., 2017. Enhanced circulating ilc2s and mdscs may contribute to ensure maintenance of th2 predominant in patients with lung cancer. Mol. Med. Rep. 15 (6), 4374–4381.

Zhang, M., Wu, W., Ren, Y., et al., 2017. Structural characterization of a novel polysaccharide from Lepidium meyenii (Maca) and analysis of its regulatory function in macrophage polarization in vitro. J. Agric. Food. Chem. 65 (6), 1146–1157.

Zhiyu, W., Wang, N., Wang, Q., et al., 2016. The inflammasome: an emerging therapeutic oncotarget for cancer prevention. Oncotarget 7 (31), 50766.